JOURNAL OF Applied Polymer SCIENCE

Preparation of a Polymer Containing Indole Groups by RAFT Polymerization and One-Phase Synthesis of AuNPs-Polymer Nanocomposites

Juan Liu,[1] Pei-Yang Gu,[1] Na-Jun Li,[1,2] Li-Hua Wang,[1,2] Chun-Yu Zhang,[1] Qing-Feng Xu,[1,2] Jian-Mei Lu[1,2]

[1]Key Laboratory of Organic Synthesis of Jiangsu Province, School of Chemistry, Chemical Engineering and Materials Science, Soochow University (DuShuHu Campus), 199 Renai Road, Suzhou, 215123, China

[2]Key Laboratory of Energy-saving and Environmental Protection Materials Test and Technical Service Center of Jiangsu Province, Soochow University (DuShuHu Campus), 199 Renai Road, Suzhou, 215123, China

Correspondence to: J.-M. Lu (E-mail: lujm@suda.edu.cn) or Q.-F. Xu (E-mail: xuqingfeng@suda.edu.cn)

ABSTRACT: A one-phase synthesis of AuNPs-polymer nanocomposites using $HAuCl_4$ as the precursor is reported in this article. A flexible polymer, poly(2-(4-(di(1*H*-indol-3-yl)methyl)phenoxy) ethyl methacrylate) (PMPEM), containing indole groups on the side chain was utilized as both a reducing reagent and soft template in the system. The PMPEM-Au nanocomposites with three different sizes of AuNPs (25–50, 2, and 5 nm) were obtained just through choosing different solvents such as toluene, tetrahydrofuran (THF), and *N*,*N*-dimethylformamide, respectively. Nanocomposites including the size of 25–50 and 2 nm AuNPs showed strong NLO absorption and refraction behaviors. The nonlinear refractive index n_2 of PMPEM-Au nanocomposites prepared in toluene and THF were 9.35×10^{-11} and 1.85×10^{-10} m^2/W, third-order susceptibility $\chi^{(3)}$ were 2.55×10^{-11} and 4.26×10^{-11} esu, respectively. © 2013 Wiley Periodicals, Inc. J. Appl. Polym. Sci. 000: 000–000, 2013

KEYWORDS: nanostructured polymers; nanoparticles; nanowires and nanocrystals; self-assembly; composites; optical properties

Received 10 December 2012; accepted 15 January 2013; published online
DOI: 10.1002/app.39026

INTRODUCTION

Nanocomposites containing gold nanoparticles (AuNPs) in polymeric matrices have been extensively studied because of the extraordinary chemical and physical properties.[1–4] The polymeric matrices can not only enhance the stability of gold cores effectively, but also functionalize the gold core due to the special properties of outside polymer layers. Such nanocomposites display potential applications in the nanocarriers for catalysts, dyes, and biosensors, as well as the fundamental building blocks for hierarchically structured materials.[5–8]

The recent reports on the preparation of nanocomposites were mainly focused on covalent linkage.[9–11] This is because the coordination of the metal cations with the ligand atoms of polymer can dramatically limit the particle size. For example, size-controlled AuNPs have been prepared by a seed-mediated growth in the presence of PVP, and the seeded clusters with a diameter of 1.3 nm have been created by reducing $AuCl_4^-$ with $NaBH_4$ in a low temperature aqueous solution.[12]

As the usual preparation of AuNPs include at least two steps: reducing and stabilizing step, a variety of amines have been used both as a reducing agent and stabilizer to simplify the process,[13–18] including simple primary amines,[17,18] amino acids,[13–15] and multifunctional amines existing in natural polymers such as DNA.[19] The reaction time is always long. Intrigued by this, we designed a monomer containing indole groups on the side chain (Scheme 1). Via RAFT polymerization, the functional polymer poly(2-(4-(di (1H-indol-3-yl) methyl) phenoxy) ethyl methacrylate) (PMPEM) with a narrow molecular weight distribution can act both as a reducing agent and stabilizer to reduce $HAuCl_4$ directly in a relatively short time. Moreover, due to the self-assembly in organic solvents, the polymer can form different sizes of microsphere and act as the soft template to reduce $HAuCl_4$ to AuNPs in different sizes. The morphology, composition, optical properties, and size were investigated in details. The third-order nonlinear optical properties of colloidal solutions of PMPEM-Au nanocomposites were also studied by using the Z-scan technique.

Additional Supporting Information may be found in the online version of this article.

Applied Polymer SCIENCE

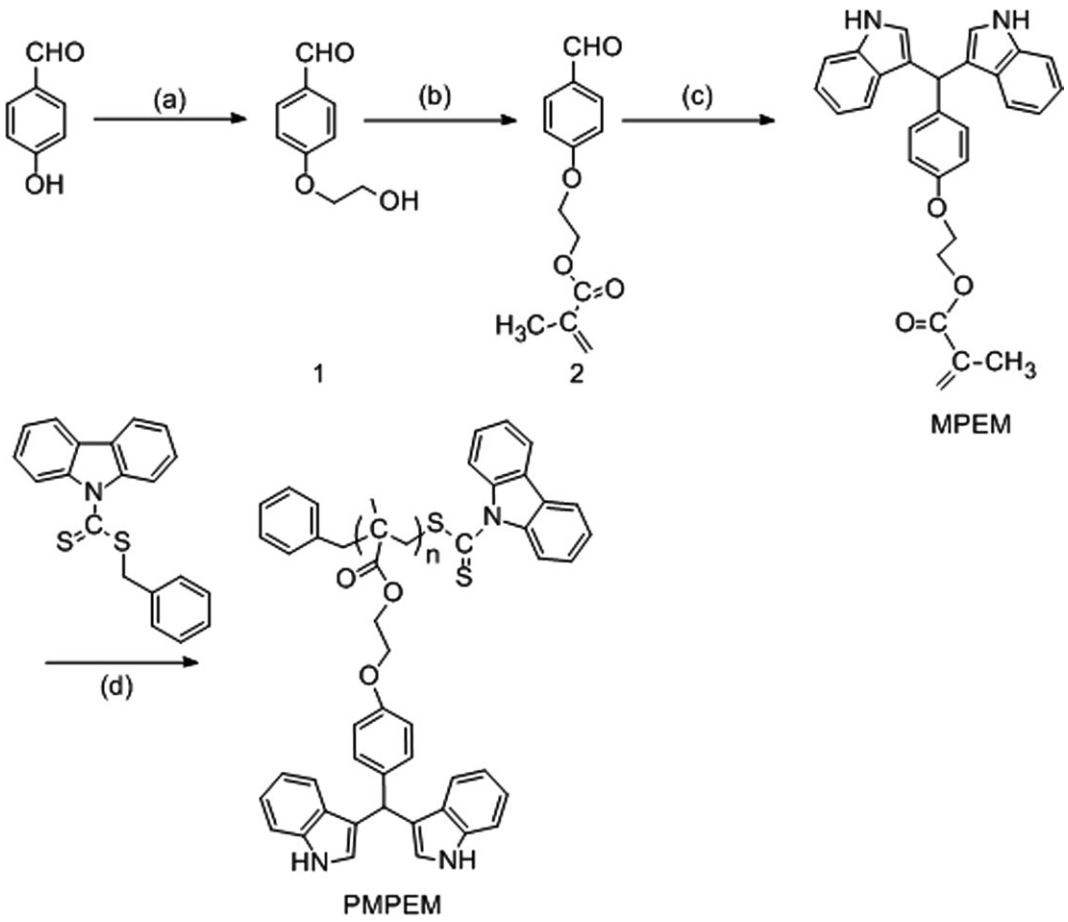

Scheme 1. Synthetic route of PMPEM. Reagents: (a) (i) $NaOH/H_2O$, (ii) C_2H_5ClO, (b) C_4H_5ClO/NEt_3, (c) indole/CAN/methanol, and (d) AIBN/cyclohexanone.

EXPERIMENTAL

Materials

Chloroauric acid tetrahydrate ($HAuCl_4$), thiethyamine (NEt_3), p-Hydroxybenzaldehyde, carbazole, indole, cerous ammonium nitrate (CAN), benzyl bromide, sodium hydroxide (NaOH), potassium hydroxide, and anhydrous magnesium sulfate ($MgSO_4$) were purchased from Shanghai Sinopharm without any further purification. Methacryloyl chloride (98%, Haimen Best Fine Chemical, Jiangsu, China) and cyclohexanone were distilled under vacuum before using. Azobisisobutyronitrile (AIBN) was recrystallized from CH_3OH. Carbon disulfide (CS_2), tetrahydrofuran (THF), toluene, *N*,*N*-dimethylformamide (DMF), dimethyl sulfoxide (DMSO), and other solvents were used as received without any further purification.

Synthesis of RAFT Chain Transfer Agent

Benzyl 9H-carbazole-9-carbodithioate (BCCT) was synthesized as described in the corresponding references.[20]

Synthesis of Monomer 2-(4-(Di(1*H*-indol-3-yl) methyl)phenoxy) Ethyl Methacrylate

Synthesis of Compound 1. *p*-Hydroxybenzaldehyde (61 g, 0.4 mol), 2-chloroethanol (48.3 g, 0.6 mol), NaOH (24 g, 0.6 mol) were mixed in deionized water (400 mL) and refluxed for 12 h in a three-necked flask. After cooling to room temperature, the solution was extracted by dichloromethane. The CH_2Cl_2 solution was washed by 10% NaOH aqueous solution three times and then dried with $MgSO_4$ overnight. Compound **1** (46 g, 55.7%) was obtained by vacuum distillation as Yellow viscous liquid.

^{1}H-NMR (300 MHz, $CDCl_3$, δ): 2.48 (s, 1H, OH), 4.01–4.03 (t, 2H, alkyl), 4.16–4.18 (t, 2H, alkyl), 7.00–7.02 (m, 2H, Ar H), 7.84–7.86 (m, 2H, Ar H) 9.88 (s, 1H, O═C─H).

Synthesis of Compound 2. A mixture of compound **1** (28 g, 0.1687 mol) and triethylamine (70 mL, 0.5061 mol)) in CH_2Cl_2 (60 mL) was stirred at room temperature. Then a solution of methylacryloyl chloride (49 mL) in dichloromethane (30 mL) was added dropwise for 1 h, and then stirred at room temperature for 6 h. After reaction, the mixture was poured into water, separated the organic layer and washed with 10% NaOH aqueous solution three times, then washed with deionized water to neutrality. The organic layer was dried with $MgSO_4$ overnight. Compound **2** (30.72 g, 74.6%) was obtained by vacuum distillation as Yellow viscous liquid.

^{1}H-NMR (300 MHz, $CDCl_3$, δ): 2.00 (s, 3H, CH_3), 4.30–4.32 (t, 2H, OCH_2CH_2O), 4.52–4.53 (t, 2H, OCH_2CH_2O), 5.68 (s, 1H, $C{=}CH_2$), 6.14 (s, 1H, $C{=}CH_2$), 7.02–7.04 (m, 2H, Ar H), 7.84–7.86 (m, 2H, Ar H), 9.89 (s, 1H,OH).

Synthesis of MPEM

A mixture of compound **2** (23.4 mg, 1 mmol), indole (23.4 mg, 2 mmol), CAN (5.5 mg, 0.1 mmol) and anydro-methanol were grounded in a mortar at room temperature for several hours to yield powder, then the solid was collected on a filter and dried. The residue was recrystallized from ethanol to afford the pure 2-(4-(di (1H-indol-3-yl) methyl) phenoxy) ethyl methacrylate (MPEM).

^{1}H-NMR (300 MHz, DMSO-d_6, δ): 10.78 (s, 2H, NH), 7.33 (d, 2H, indole H), 7.25 (t, 4H, indole H), 7.02 (t, 2H, indole H), 6.86 (d, 4H, Ar H and indole H), 6.78 (d, 2H, indole H), 6.01 (s, 1H, C=CH_2), 5.76 (s, 1H, C=CH_2), 5.66 (s, 1H, CH), 4.39 (d, 2H, OCH_2CH_2O), 4.19 (d, 2H, OCH_2CH_2O), 1.86 (s, 3H, CH_3).

Polymerization of MPEM by RAFT Polymerization

The PMPEM was synthesized via RAFT polymerization technique. The typical polymerization procedure was as follows: monomer MPEM, BCCT and AIBN in a molar ratio of 200 : 6 : 1 were dissolved in cyclohexanone in a dried flask. The solution was exposed to nitrogen bubbling for 20 min to deoxidate, and polymerization was processed at 60°C. After 2 h, the solution was cooled down in ice water. The reacted mixture was poured into methanol. The polymer was purified by dissolution in THF and precipitated from methanol for three times. The purified products were dried under vacuum at room temperature.

Synthesis of PMPEM-Au Nanocomposites

PMPEM-AuNP^1. A mixture of PMPEM (2.4 mg), THF (0.5 mL), and toluene (12 mL) was heated at reflux for 0.5 h in a three-necked flask at 120°C. Then a toluene solution of $HAuCl_4$ (1 mg/mL) was added into the mixture. The amount of $HAuCl_4$ in toluene solution and reaction time were varied from 120 to 480 μL and 40–120 min, respectively.

PMPEM-AuNP^2. PMPEM (2.4 mg) was dissolved in THF (12 mL) while refluxing for 0.5 h in a three-necked flask at 60°C. Then 480 μL of a $HAuCl_4$ (1 mg/mL) in THF was added into the solution with continuous stirring for 40 min.

PMPEM-AuNP^3. PMPEM (2.4 mg) was dissolved in DMF (12 mL) while refluxing for 0.5 h in a three-necked flask at 120°C. Then 480 μL of a $HAuCl_4$ (1 mg/mL) in DMF was added into the solution with continuous stirring for 40 min. The products were centrifugated at 3000 rpm for 10 min and washed with ethanol for several times to remove the excess PMPEM.

Characterization

^{1}H-NMR spectra were measured on an INOVA 300 MHz NMR spectrometer, using $CDCl_3$ or DMSO-d_6 as solvent and tetramethylsilane as the internal standard at ambient temperature. Wide-angle X-ray diffraction (XRD) patterns were taken on an X'Pert-Pro MPD X-ray diffractometer. FT-IR spectra measurement was performed as KBr pellets on a Perkin-Elmer 577 FT-IR spectrometer in the range of 400–4000 cm^{-1}. Thermal gravimetric analysis (TGA) was conducted on a Universal V3.7ATA instrument under flowing pure N_2 gas (50 mL/min) at a heating rate of 10°C/min from room temperature to 800°C. UV–vis was measured on a Perkin–Elmer λ-17 UV photometer between 250 and 700 nm. The fluorescence spectra were measured on Edinburgh-920 fluorescence spectra photometer (Edinburgh Co., UK) with a slit of 5 nm. Molecular weights and the polydispersity relative to PMPEM were measured using Waters1515 GPC with DMF as a mobile phase at a flow rate of 1 mL/min and with column temperature of 30°C. Room temperature emission and excitation luminescent spectra were carried out by using Edinburgh-920 fluorescence spectra photometer. TEM imagination and Energy Dispersive X-ray (EDX) of the samples were carried out with a FEI TecnaiG220 microscope working at 200 kV. The third-order NLO properties were measured by the Z-scan technique and based on the transformation of phase distortion during beam propagation.

RESULTS AND DISCUSSION

Characterization of Monomer and Polymer

Structures of monomer and polymer are presented in Scheme 1. PMPEM had a molecular weight (Mn) of 23,800 with a polydispersity index of 1.28 as determined by GPC, which is in the expected range for RAFT polymerization. Supporting Information Figure S1 exhibits the ^{1}H-NMR spectra of PMPEM and monomer in which the signals of hydrogen atom from the vinyl group (5.5–6.0 ppm) were disappeared and a broad signal of methylene below 2.0 ppm was appeared. Hence, the ^{1}H-NMR spectrum along with GPC results indicates the successful synthesis of PMEPM. The PMPEM also exhibits good thermal stability, with a glass transition temperature about 168°C (Supporting Information Figure S2) and an onset decomposition temperature about 34°C (Figure 4) determined by differential scanning calorimetry and thermogravimetric analysis respectively.

Morphology and Formation Mechanism

Similar to oleylamine,[21–22] PMPEM containing indole groups can reduce Au (III) ion to AuNPs. In our reaction system, $HAuCl_4$ solution was added to the PMPEM solution while stirring. Gradually, the initially canary yellow solution turned to red, indicating the reduction of Au (III) to the Au^0 state. AuNPs could be electrostatically attracted on the surface of PMPEM, forming PMPEM-Au nanocomposites. Our system is unique because the PMPEM-Au nanocomposites were directly obtained from the mixture of functional polymer and $HAuCl_4$ just in one step (Figure 1).

In the reaction system, PMPEM was used as both reductant and template simultaneously.[23] The reaction time was about 40 min and the size of AuNPs can be controlled by changing the solvent. According to the solubility in different solvents, polymer coil of PMPEM can self-assemble into spherical micelles when diffusing in toluene and THF[24–27] (Figure 2). Because of the better solubility of PMPEM in THF, the size of micelles was obviously smaller than that in toluene. The diameter of the spherical micells in the toluene was about 300 nm, and the interacted micells in the THF was about 150 nm. The spherical micelles in the reaction solution acted as soft templates. Indole cations have strong affinity with AuNPs by electrostatic effects due to the electronegativity of the surface of the AuNPs. As a result, the micells were modified with a number of tiny spherical AuNPs on surface. This coating of nanoparticles is analogous to the previous report.[28]

Applied Polymer SCIENCE

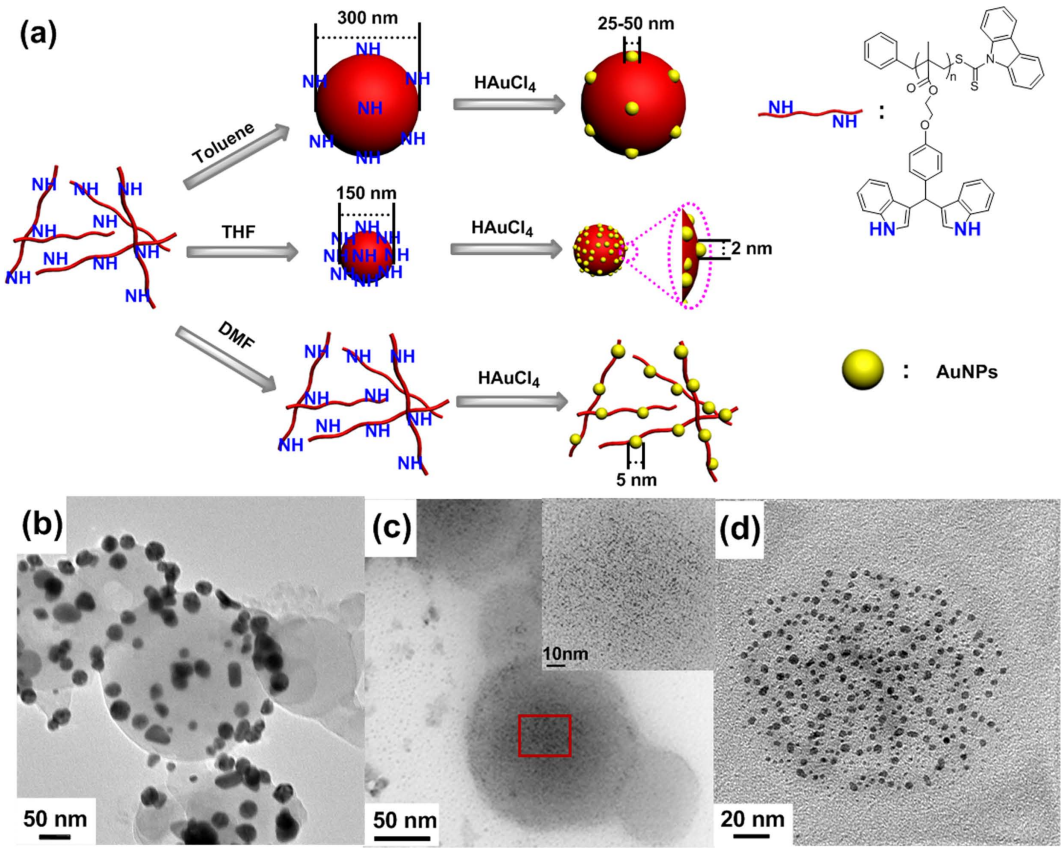

Figure 1. Transmission electron microscope images of PMPEM-Au nanocomposites. (a) PMPEM-AuNP[1] (25–50 nm AuNPs from toluene), (b) PMPEM-AuNP[2] (~2 nm AuNPs from THF), (c) PMPEM-AuNP[3] (~5 nm AuNPs from DMF). [Color figure can be viewed in the online issue, which is available at wileyonlinelibrary.com.]

In toluene, imido groups on micelles surface are relatively less due to its poor solubility and affinity to oleophilic solvent. We chose two reaction temperatures 60 and 120°C to observe the growth of AuNPs. The reaction was first performed in toluene at 60°C, gold nanoparticles formed more slowly and the size was relatively smaller (Supporting Information Figure S3) compared to the AuNPs formed at 120°C in toluene.[29] At 120°C, gold particles were grown in situ. Different-shaped nano-crystals with a size distribution of 25–50 nm can be observed in Figure 1(b).

In THF, imido groups on the micelle surface are more than that in toluene. When the reaction was performed at 60°C, the size of formed gold nanoparticles was relatively smaller. We obtained PMPEM-AuNP[2] with ~2 nm AuNPs on the surface of spherical micelles in THF as shown in Figure 1(c). It is known that Au

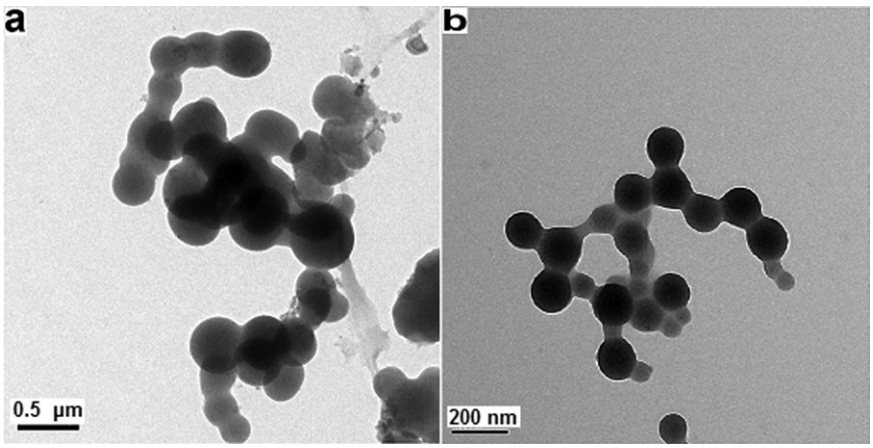

Figure 2. Transmission electron microscope images of PMEPM when diffusing in (a) toluene and (b) THF.

nanoparticles less than 3 nm in size do not exhibit the characteristic peak of surface plasmon resonance at around 520 nm.[30,31] The spherical micelles clustered together and the AuNPs were so small that we characterized them by EDX (Supporting Information Figure S4). EDX spectra further confirmed the presence of gold (Au) in the sample.

DMF is a good solvent for PMPEM, which means higher concentration of reducing agents (imido groups) in the DMF solution when PMPEM was dissolved in. In the homogeneous system, the formation and growth of particles were affected by the wrapping of polymer chains,[32] resulting in nearly monodispersed PMPEM-AuNP^3 with core diameters of ~5 nm [Figure 1(d)].

XRD

Figure 3 shows the XRD patterns of (a) PMPEM, (b) PMPEM-AuNP^1 prepared in toluene, and (c) PMPEM-AuNP^3 prepared in DMF. In Figure 3(b,c), four additional peaks at 38.62°, 44.80°, 64.93°, and 77.8° that represented Bragg's reflections from (111), (200), (220), and (311) planes of Au were observed besides the peaks of PMPEM, which indicated the existence of Au nanoparticles in the composites. The average size of nanoparticles was estimated based on Scherrer correlation of particle diameter (D) with peak width (As, full width at half maximum, $\lambda = 0.154$ nm) for Bragg diffraction from ideal single domain crystallites $D = K\lambda/(\beta \cos \theta)$, where K is the Scherrer constant (0.89), θ is the diffraction angle, β is the half width at half-maximum.

According to the Scherrer equation, the average size of the Au particles calculated from the width of the diffraction peak was ~25 nm [Figure 3(b)] and ~5 nm [Figure 3(c)], respectively, in accordance with the TEM. The Au NPs less than 3 nm in size prepared from THF did not show the diffraction features.

Thermogravimetric Analysis

Thermogravimetric analysis (TGA) was employed to determine the relative content of each component in PMPEM-Au nanocomposites (Figure 4). The residual mass percent refers to the mass percentage of Au in the composite. As shown in the TGA curve, there was a small amount of weight loss below 130°C due to the evaporation of water. The total weight loss of pure PMPEM was 100% under these experimental conditions. The contents of AuNPs should amount to 12.1% in the polymer matrix if all the Au ions were reduced during the preparation of the PMPEM-Au nanocomposites. The contents of inorganic Au prepared in toluene, THF and DMF are 11.5, 7.5, and 10.9%, respectively.

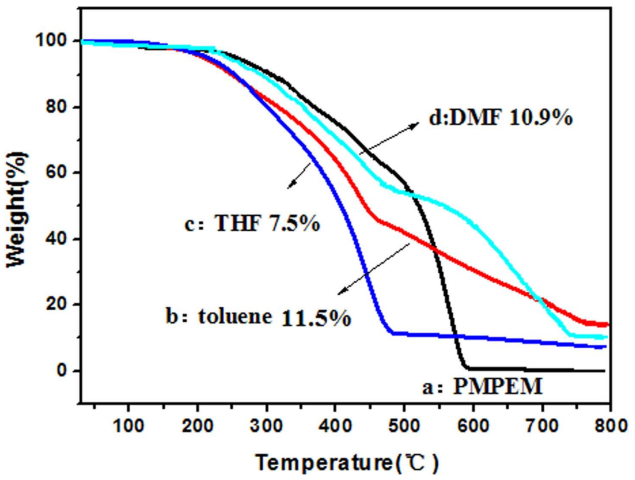

Figure 4. TGA thermograms of (a) PMPEM, (b) PMPEM-AuNP^1, (c) PMPEM-AuNP^2, and (d) PMPEM-AuNP^3. The thermograms were obtained at a scan rate of 10°C/min under nitrogen flow. [Color figure can be viewed in the online issue, which is available at wileyonlinelibrary.com.]

FTIR Spectra

Figure 5 illustrates the FT-IR spectra of the prepared pure PMPEM and PMPEM-Au nanocomposites in three different organic solvents. The bands at 1608, 1509, and 1420 cm^{-1} were

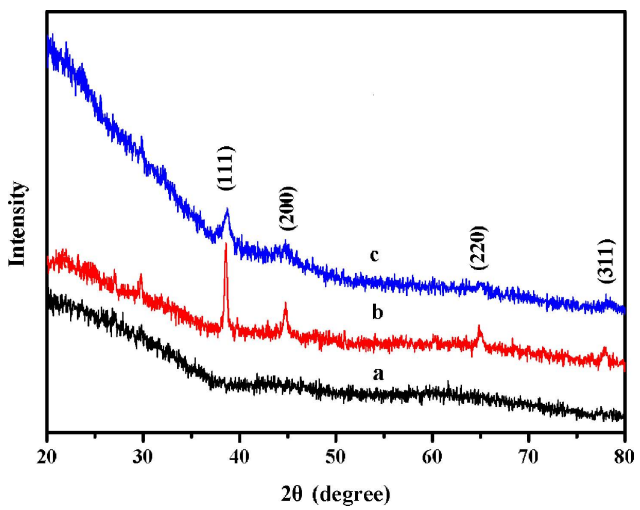

Figure 3. X-ray power diffraction patterns of (a) PMPEM, (b) PMPEM-AuNP^1, and (c) PMPEM-AuNP^3. [Color figure can be viewed in the online issue, which is available at wileyonlinelibrary.com.]

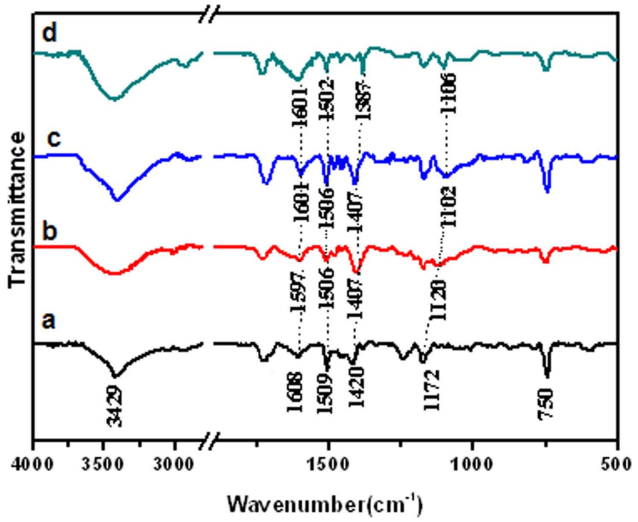

Figure 5. FT-IR spectra of (a) PMPEM, (b) PMPEM-AuNP^1, (c) PMPEM-AuNP^2, and (d) PMPEM-AuNP^3. [Color figure can be viewed in the online issue, which is available at wileyonlinelibrary.com.]

attributed to the stretching vibration modes of C=C and C—C in the benzene ring, and the band around 750 cm^{-1} is due to the bending vibration mode of benzene ring. The stretching vibration mode of the N—H bond could be seen at 3429 cm^{-1}. A significant blue-shift of the adsorption peaks occurred when PMPEM was combined with Au. The shift to lower energy suggested that Au, as the electron donator, made the electron cloud of PMPEM more delocalized, similar to the phenomenon that reported in polyaniline combining with AuNPs.[23,33] The C—N stretch shifted from 1172 to 1120 cm^{-1}, indicating the interaction between C—N bonds (or amino and imino bonds) of the polymer and the gold nanoparticles. Au donated electron density to the imino nitrogen in the polymer. It was interesting to note that no large change in the energy for the N—H band was observed (3429 cm^{-1}). It may be due to that the electron density of the C—N bond suffered greater effect from the gold particles present in the PMPEM matrix.[34]

UV–Vis Spectra and Fluorescence Spectra

Figure 6 exhibits the characteristic UV–vis absorption of Au nanoparticles prepared in three different organic solvents. Curves b–d corresponded to the samples prepared in toluene, THF and DMF, respectively. The ligand PMPEM showed one absorption band at 286 nm, assigned to π–π^* transition. In Figure 3(b), absorption at 510 nm was due to the surface plasmon resonance of AuNPs. The surface plasmon resonance band of gold colloids is calculated theoretically to be at 510–525 nm.[35] But in our system, the absorptions were at 430 and 500 nm, which resulted from the HCl formed in the reaction. The two peaks were too strong to show the absorption character of AuNPs.

The emission spectra of samples dissolved in toluene excited at 294 nm was shown in Figure 7. The broad emission peak at 342 nm resulted from the π–π^* transition of PMPEM. As we know, AuNPs are capable of quenching proximal fluorophores.[36] AuNPs serve as an efficient quencher of the polymer excitonic fluorescence (excimer peak), presumably through long-range resonance energy transfer. Therefore, by adding $HAuCl_4$ into the toluene solution of PMPEM, the intensity of emission peak was significantly reduced, in line with the energy transfer of absorption band on nanoparticles.[37] The time-dependent fluorescent changes of the reaction mixture were recorded at 0, 40, 80, and 120 min after the injection of $HAuCl_4$ to the toluene solution of PMPEM. The decrease of fluorescence was proportional to the content of AuNPs, meaning that more $AuCl_4^-$ have been reduced to the Au^0 state by PMPEM gradually with the prolonged reaction time.

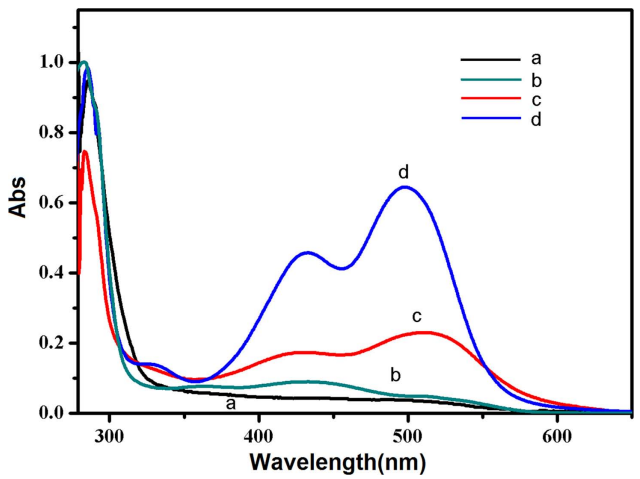

Figure 6. UV–vis spectra recorded from the gold colloids prepared in three different organic solvent (a) PMPEM, (b) PMPEM-$AuNP^1$, (c) PMPEM-$AuNP^2$, and (d) PMPEM-$AuNP^3$. [Color figure can be viewed in the online issue, which is available at wileyonlinelibrary.com.]

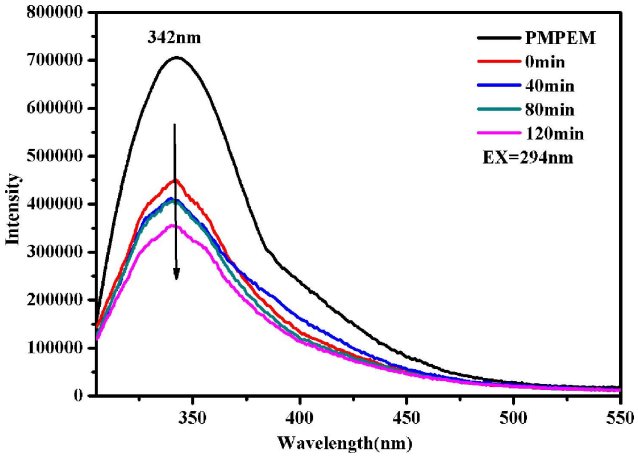

Figure 7. Fluorescence spectra obtained during the formation of AuNPs at different time intervals after the addition of $HAuCl_4$ to the toluene solution of PMPEM. [Color figure can be viewed in the online issue, which is available at wileyonlinelibrary.com.]

We have further proven the formation of AuNPs in toluene by varying the amount of $HAuCl_4$ to the toluene solution of PMPEM. There was no significant absorption at about 532 nm after addition of 180 μL $HAuCl_4$ in toluene [Supporting Information Figure S5(a)]. With more $HAuCl_4$ added in, the absorption peak emerged at around 500 nm. This emerged peak red-shifted gradually, indicating the generation of more AuNPs. The red shift and broadening of the Plasmon absorption band also meant the increase of particle size and its wide polydispersity.[38] The AuNPs on the surface of PMPEM spherical colloids effectively quenched the intrinsic fluorescence of the PMPEM, thus further highlighted the strong interaction between the two components. With the amount of $HAuCl_4$ continuing to increase, fluorescence was gradually quenched [Supporting Information Figure S5(b)].

Fluorescence Emission Spectra of PMPEM-$AuNP^2$ in THF

It was well known that gold nanoclusters (GNCs) have attracted wide attention owing to their outstanding surface and physical properties such as near-infrared photoluminescence.[39–41] Figure 8 depicts the fluorescence emission spectra of PMPEM-$AuNP^2$ in THF. Excited by 490 nm light, the steady-state fluorescence spectrum of PMPEM-$AuNP^2$ displayed an emission peak at 615 nm, coincide with the reported fluorescence emission bands of GNCs.[42] The result demonstrated the formation of ~2 nm AuNPs in THF.

Nonlinear Optical Properties

Nanocomposite materials, particularly of metal nanoparticles doped organic polymer nanocomposites, have been widely

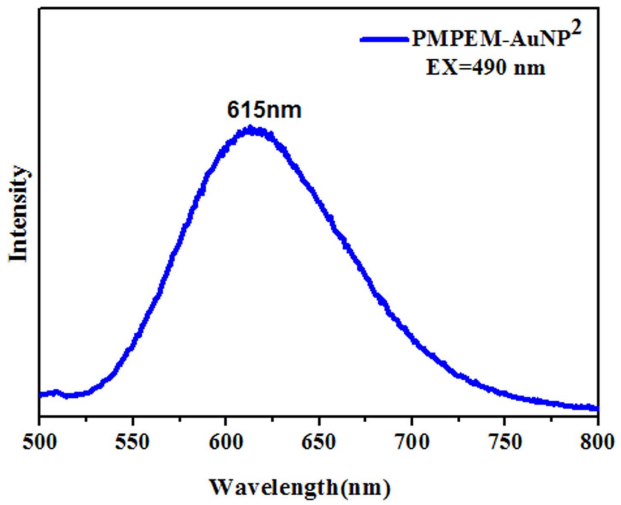

Figure 8. Fluorescence emission spectra of PMPEM-AuNP^2 (λ_{Ex} = 490 nm) in THF. [Color figure can be viewed in the online issue, which is available at wileyonlinelibrary.com.]

studied because of the potential applications in optical switching, light-controlled phase and optical power limiting devices.[43–45] By incorporating metal nanoparticles into a polymer matrix, the nanocomposites will exhibit specific optical absorption and large third-order optical nonlinearity different from bulk materials. The optical properties of nanocomposite materials can be judiciously tuned by adjusting the particle size and spacing. The third-order nonlinear optical properties of PMEPM-Au nanocomposites with different sizes of AuNPs were measured via the Z-Scan method. The Z-Scan method chooses Nd: YAG nanosecond laser as the light source, which owns a wavelength of 532 nm, a pulse width of 4 ns and a repetition rate of 10 Hz. The thickness of the sample cell is 2 mm. The measurement can be performed through closed aperture and open aperture configurations.

Under the same conditions, PMPEM alone had no nonlinear absorption. The 5 nm AuNPs prepared in DMF hardly limited light absorption even at very high fluency of nanosecond laser pulses, similar as a previous report by Mostafavi and co-workers.[46] In contrast, the PMPEM-Au nanocomposites prepared in toluene [Figure 9(A)] and THF [Figure 9(B)] showed large nonlinear optical response. Figure 9 shows the Z-scan measurement data with the open aperture and closed aperture, containing both contributions from the nonlinear absorption and nonlinear refractive index. The open-aperture Z-scan curves [Figure 9A(a), B(a)] both showed reverse-saturated absorption, which were induced by nonlinear scattering. Figure 9A(b), 9B(b) shows the normalized transmittance versus the sample position after the closed-aperture Z-scan divided by the open-aperture Z-scan. The curves exhibited a valley-to-peak profile, indicating a positive value of the nonlinear refractive index n_2, which characterized the self-focusing property of the sample

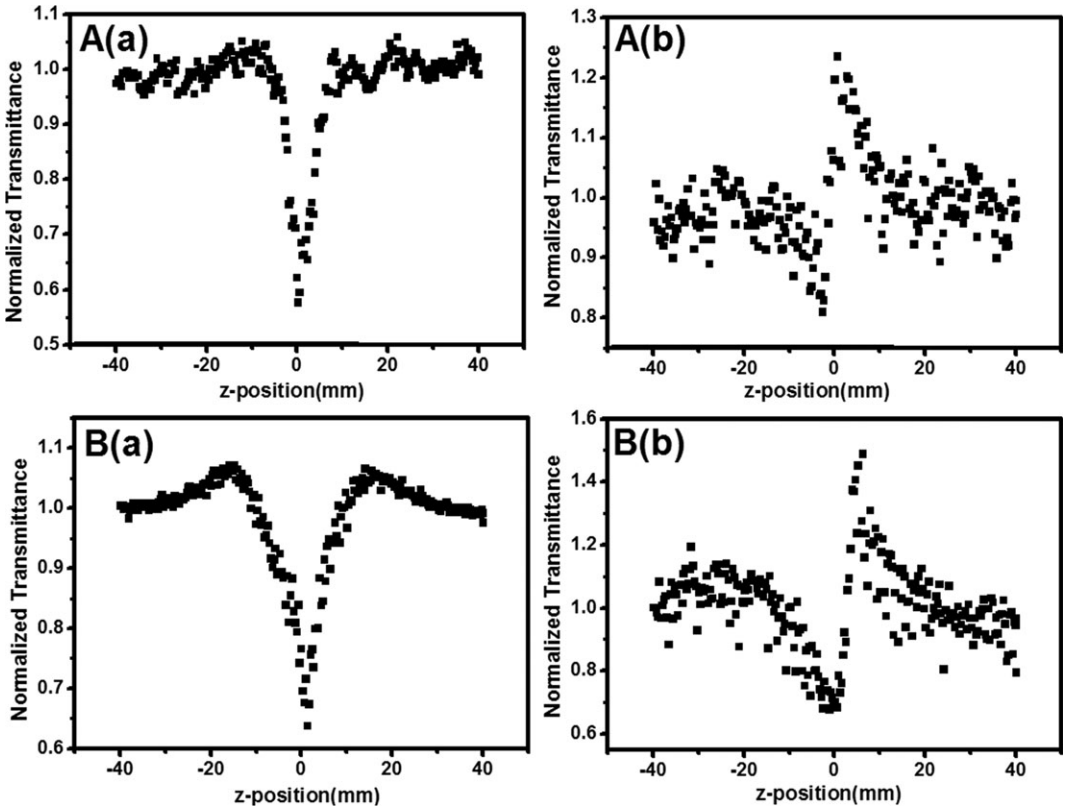

Figure 9. The normalized energy transmissions of Z-scan experiments with open aperture A (a), B (a) and closed aperture A (b), B (b) for PMPEM-AuNP^1 in toluene and PMPEM-AuNP^2 in THF. The NLO properties of the samples were investigated under a wavelength of 532 nm and a pulse width of 4 ns using Nd: YAG laser.

Table I. The Third-Order Nonlinearity of PMPEM-Au Nanocomposites Prepared in Three Different Organic Solvent

Sample	Size of AuNPs (nm)	T_0[a] (%)	E[b] (μJ)	β[c] (10^{-10} MKS)	n_2[d] (10^{-11} m^2/W)	$\chi^{(3)}$[e] (10^{-11} esu)
PMPEM-AuNP[1]	25–50	64	10.04	3.4	9.35	2.6
PMPEM-AuNP[2]	2	62	9.35	3.2	18.5	4.3
PMPEM-AuNP[3]	5	65	15.38	0	0	0

[a]The linear transmittance.
[b]The energy in measurement.
[c]Nonlinear absorption coefficient.
[d]Nonlinear refractive index.
[e]Third-order susceptibility.

under investigation. The asymmetry of the closed aperture Z-scan curve also pointed to the presence of nonlinear absorption.

According to Z-scan theory,[47] the nonlinear refractive index n_2 is related to ΔT_{p-v} as $n_2 = \Delta T_{p-v}\ \lambda\alpha/[0.812\pi I_0(1 - \exp(-\alpha L))]$, where ΔT_{p-v} is the difference between the normalized peak and valley transmittances of the apertured Z-scan, λ is the laser wavelength (532 nm), α is the linear absorption coefficient, $\alpha = \beta(I_i)$; I_0 is the pulse irradiance, $I_0 = E/(\pi\omega^2\tau)$, where E is the laser energy; ω is the radius of laser beam, 25 μm; t is the pulse width, 4 ns; L is the sample thickness, 2 mm. Although the third-order susceptibility $\chi^{(3)}$ is linked to n_2 through $\chi^{(3)} = 4/3\varepsilon_0 c{n_0}^2 \times n_2$, where ε_0 is the vacuum permittivity, 8.85×10^{-12} F/m); c is the light speed in vacuum, 3×10^8 m/s; n_0 is the linear refractive index of the medium, which we approximate here to the n_0 (toluene: 1.497, THF: 1.407, DMF: 1.426) value of the solvent. The detailed parameters of the NLO properties of the PMPEM-Au nanocomposites were presented in Table I. As shown in Table I, the n_2 of PMPEM-Au nanocomposites prepared in toluene and THF were 9.35×10^{-11} and 1.85×10^{-10} m^2/W, respectively. The third-order susceptibility $\chi^{(3)}$ of PMPEM-Au nanocomposites prepared in toluene and THF were 2.55×10^{-11} and 4.26×10^{-11} esu, which are larger than the reported values of P3DDT–CdS nanocomposite (4.41×10^{-12} esu) prepared by a chemically hybridized approach.[48] The obtained values are also two orders of magnitude greater than porphyrin alkanethiol capped Au nanoparticles in toluene solution (0.9×10^{-13} esu).[49] The third-order susceptibility $\chi^{(3)}$ of Au/PVA-PVP and Ag/PVA-PVP thin films obtained under similar excitation conditions are 3.6×10^{-11} esu and 2.36×10^{-11} esu, respectively.[50] Therefore, the PMPEM-Au nanocomposites can be used as an optical limiting material. The incorporation of metal nanoparticles into the polymer matrix could be a promising method to obtain polymeric materials with high nonlinear response. It would be useful in developing nonlinear optical devices applied in an extended region.

CONCLUSIONS

In this study, we have shown a facile method to prepare different-sized Au nanoparticles. The particle size was able to be readily solvent-controlled. The content of Au nanoparticles in the nanocomposites was determined by TGA. The FT-IR absorption peaks of PMPEM-Au nanocomposites blue-shifted compared to that of pure PMPEM. XRD measurements indicated the presence of Au in the composites. The high temperature and poor solvent of polymer produced larger Au particles with wide size distribution, or vice versa. This unique synthetic strategy allowed different sizes of gold nanoparticles to be prepared in a remarkable yield without requiring any post-synthesis treatments. Moreover, the PMPEM-Au nanocomposites showed large nonlinear optical response. The n_2 of PMPEM-Au nanocomposites prepared in toluene and THF were $9.35 \times 10^{-11}$and 1.85×10^{-10} m^2/W, the third-order susceptibility $\chi^{(3)}$ were 2.55×10^{-11} and 4.26×10^{-11} esu, respectively. The results showed that the nanocomposites have potential use in nonlinear optical devices.

ACKNOWLEDGMENTS

The authors thank the Chinese Natural Science Foundation (21071105 and 21176164), the National Key Technology R&D Program (2012BAC14B03), and the Project of Science and Technology of Suzhou (SYG201114).

REFERENCES

1. Boisselier, E.; Astruc, D. *Chem. Soc. Rev.* **2009**, *38*, 1759.
2. He, Q.; Kueller, A.; Schilp, S.; Leisten, F.; Kolb, H. A.; Grunze, M.; Li, J. B. *Small* **2007**, *3*, 1860.
3. Bunz, U. H. F.; Rotello, V. M. *Angew. Chem. Int. Ed. Engl.* **2010**, *49*, 3268.
4. Li, J.; Song, S. P.; Liu, X. F.; Wang, L. H.; Pan, D.; Huang, Q.; Zhao, Y.; Fan, C. H. *Adv. Mater.* **2008**, *20*, 497.
5. Kim, D. J.; Kang, S. M.; Kong, B.; Kim, W. J.; Paik, H. J.; Choi, H.; Choi, I. S. *Macromol. Chem. Phys.* **2005**, *206*, 1941.
6. Ge, Z. B.; Kang, Y. J.; Taton, T. A.; Braun, P. V.; Cahill, D. G. *Nano Lett.* **2005**, *5*, 531.
7. Anna, C. B.; Todd, E.; Thomas, P. R. *Science* **2006**, *314*, 1107.
8. Ohno, K.; Morinaga, T.; Koh, K.; Tsujii, Y.; Fukuda. T. *Macromolecules* **2005**, *38*, 2137.
9. Corbierre, M. K.; Cameron, N. S.; Lennox, R. B. *Langmuir* **2004**, *20*, 2867.
10. Zhu, M. Q.; Wang, L. Q.; Exarhos, G. J.; Li, A. D. Q. *J. Am. Chem. Soc.* **2004**, *126*, 2656.
11. Li, D. X.; Cui, Y.; Wang, K. W.; He, Q.; Yan, X. H.; Li, J. B. *Adv. Funct. Mater.* **2007**, *17*, 3134.
12. Tsunoyama, H.; Sakurai, H.; Tsukuda, T. *Chem. Phys. Lett.* **2006**, *429*, 528.

13. Selvakannan, P. R.; Mandal, S.; Phadtare, S.; Gole, A.; Pasricha, R.; Adyanthaya, S. D.; Sastry, M. *J. Colloid Interface Sci.* **2004**, *269*, 97.
14. Bhargava, S. K.; Booth, J. M.; Agrawal, S.; Coloe, P.; Kar, G. *Langmuir* **2005**, *21*, 5949.
15. Aslam, M.; Fu, L.; Su, M.; Vijayamohanan, K.; Dravid, V. P. *J. Mater. Chem.* **2004**, *14*, 1795.
16. Jieun, S.; Dukhan, K.; Dongil, L. *Langmuir* **2011**, *27*, 13854.
17. Leff, D. V.; Brandt, L.; Heath, J. R. *Langmuir* **1996**, *12*, 4723.
18. Subramaniam, C.; Tom, R. T.; Pradeep, T. *J. Nanopart. Res.* **2005**, *7*, 209.
19. Chen, C. L.; Rosi, N. L; *J. Am. Chem. Soc.* **2010**, *132*, 6902.
20. Hua, D.; Zhang, J.; Bai, R.; Lu, W.; Pan, C. *Macromol. Chem. Phys.* **2004**, *205*, 1125.
21. Aslam, M.; Fu, L.; Su, M.; Vijayamohanan, K.; Dravid, V. P. *J. Mater. Chem.* **2004**, *14*, 1795.
22. Hilgendorff, M.; Liz-Marzn, L. M.; Giersig, M. *Langmuir* **2008**, *24*, 9855.
23. Feng, X. M.; Yang, G.; Xu, Q.; Hou, W. H.; Zhu, J. J. *Macromol. Rapid Commun.* **2006**, *27*, 31.
24. Shen, H. W.; Zhang, L. F.; Eisenberg, A. *J. Am. Chem. Soc.* **1999**, *121*, 2728.
25. Kim, C.; Lee, S. C.; Kang, S. W. *Langmuir* **2000**, *16*, 4792.
26. Bhargava, P.; Tu, Y. F.; Zheng, J. X. *J. Am. Chem. Soc.* **2007**, *129*, 1113.
27. Choucair, A.; Eisenberg, A. *J. Am. Chem. Soc.* **2003**, *125*, 11993.
28. Gittins, D. I.; Caruso, F. *J. Phys. Chem. B.* **2001**, *105*, 6846.
29. Chen, C. L.; Rosi, N. L. *J. Am. Chem. Soc.* **2010**, *132*, 6902.
30. Yang, X.; Xu, M.; Qiu, W.; Chen, X.; Deng, M.; Zhang, J.; Iwai, H.; Watanabe, E.; Chen, H. *J. Mater. Chem.* **2011**, *21*, 8096.
31. Zhou, R. J.; Shi, M. M.; Chen, X. Q.; Wang, M.; Chen, H. Z. *Chem. Eur. J.* **2009**, *15*, 4944.
32. Yamamoto, M.; Nakamoto, M. *J. Mater. Chem.* **2003**, *13*, 2064.
33. Zhang, H.; Zhong, X.; Xu, J. J.; Chen, H. Y. *Langmuir* **2008**, *24*, 13748.
34. Kinyanjui, J. M.; Hatchett, D. W. *Chem. Mater.* **2004**, *16*, 3390.
35. Creighton, J. A.; Eadon, D. G. *J. Chem. Soc., Faraday Trans.* **1991**, *87*, 3881.
36. Deng, S.; Advincula, R. *Chem. Mater.* **2002**, *14*, 4073.
37. Taranekar, P.; Baba, A.; Fulghum, T. M.; Advincula, R. *Macromolecules* **2005**, *38*, 3679.
38. Fleming, D. A.; Williams, M. E. *Langmuir* **2004**, *20*, 3021.
39. Peyser, L. A.; Vinson, A. E.; Bartko, A. P.; Dickson, R. M. *Science* **2001**, *291*, 103.
40. Zheng, J.; Dickson, R. M. *J. Am. Chem. Soc.* **2002**, *124*, 13982.
41. Häkkinen, H.; Abbet, S.; Sanchez, A.; Heiz, U.; Landman, U. *Angew. Chem.* **2003**, *115*, 1335.
42. Wang, C. S.; Li, J. Y.; Amatore, C.; Chen, Y.; Jiang, H.; Wang, X. M. *Angew. Chem. Int. Ed.* **2011**, *50*, 1.
43. Yuwono, A. H.; Xue, J.M.; Wang, J.; Elim, H. I.; Ji, W.; Li, Y.; White, T. J. *J. Mater. Chem.* **2003**, *13*, 1475.
44. Kurian, P. A.; Vijayan, C.; Sathiyamoorthy, K.; Suschand Sandeep, C. S.; Philip, R. *J. Nanoscale Res. Lett.* **2007**, *2*, 561.
45. Polavarapu, L.; Venkatram, N.; Ji, W; Xu, Q. H. *Appl. Mater. Interfaces.* **2009**, *1*, 2298.
46. Francois, L.; Mostafavi, M.; Belloni, J.; Delouis, J. F.; Delaire, J.; Feneyrou, P. *J. Phys. Chem. B* **2000**, *104*, 6133.
47. Ji, W.; Elim, H. I.; He, J.; Fitrilawati, F.; Baskar, C.; Valiyaveettil, S.; Knoll, W. *J. Phys. Chem. B* **2003**, *107*, 11043.
48. Dong, Y. M.; Lu, J. M.; Ji, S. J.; Lu, C.J. *Synthetic Metals.* **2011**, *161*, 2441.
49. Ouyang, C.; Liu, H. B.; Song, Y. L. *J. Nanosci. Nanotechnol.* **2012**, *12*, 2990.
50. Sudheesh, P.; Sharafudeen, K. N.; Vijayakumar, S.; Chandrasekharan, K. *J. Opt.* **2011**, *40*, 193.